Polymer photochemistry at the EUV wavelength

Citation: Theodore H. Fedynyshyn, Russell B. Goodman, Alberto Cabral, Charles Tarrio and Thomas B. Lucatorto, "Polymer photochemistry at the EUV wavelength", Proc. SPIE 7639, 76390A (2010); doi:10.1117/12.845997 © 2010 COPYRIGHT SPIE

As Published: http://dx.doi.org/10.1117/12.845997

Publisher: SPIE

Persistent URL: http://hdl.handle.net/1721.1/60941

Version: Final published version: final published article, as it appeared in a journal, conference proceedings, or other formally published context

Polymer Photochemistry at the EUV Wavelength

Theodore H. Fedynyshyn, Russell B. Goodman, Alberto Cabral, Charles Tarrio[#] and Thomas B. Lucatorto[#]

Lincoln Laboratory, Massachusetts Institute of Technology, Lexington, MA 02420
National Institute of Standards and Technology, Gaithersburg, MD 20899

ABSTRACT

The higher energy associated with extreme ultraviolet (EUV) radiation coupled with the high absorptivity of most organic polymers at these wavelengths should lead to increased excited state population and higher quantum yields of photoproducts. Polymers representative of those commonly employed in resists as well as some model polymers were selected for this study. Polymer photochemistry at EUV was catalogued as to the effect of absorbed 13.4-nm radiation on a polymer's quantum yield of chain scission (Φ_s) and crosslinking (Φ_x). In selected cases, the chain scission and crosslinking quantum yields were also compared to those previously determined at 157-, 193- and 248-nm. It was found that quantum yield values were over a magnitude greater at EUV relative to optical wavelengths.

Keywords: Photoresist, polymer photochemistry, EUV

1. INTRODUCTION

Extreme ultraviolet (EUV) lithography is being developed as a potential successor to 193 nm lithography for printing the smallest microprocessor features.[1] Resists developed for EUV lithography are typically based on modifications to materials or formulations developed for other lithographic exposures, specifically 248 nm, 193 nm, and e-beam.[2] Although much is known about the actinic radiation-induced chemistry at traditional advanced lithographic optical wavelengths (157 to 248 nm), little work has been performed at the 13.4 nm wavelength used for EUV. We recently showed that with EUV exposure, the polymer matrix was found to have a significant effect on the acid generation efficiency of the photoacid generator (PAG) studied.[3] A linear relationship exists between the absorbance of the resist and the acid generation efficiency implying polymer sensitization. Surprisingly, an inverse relationship exists between acid generation efficiency (Dill C) and aromatic content of the resist polymer that is independent of absorbance, which implies that additional polymer based photochemistry occurs that influences acid generation.

We have previously developed a gel permeation chromatography (GPC) based method to determine quantum yields for chain scission and crosslinking of thin polymer films coated on silicon wafers. This method was applied to determine the polymer's quantum yield of chain scission (Φ_s) and crosslinking (Φ_x) for a number of lithographically significant homopolymers and copolymers at 157, 193 and 248 nm wavelengths. It was found that polymers containing hydroxystyrene only undergo crosslinking while acrylate and methacrylate polymers only undergo chain scission.[4,5] We are now extending this technique to determine the Φ_s and Φ_x of a series of model polymers exposed to EUV.

Polymer photochemistry depends on photon absorption, which leads to the production of an excited electronic state of the polymer. If the excitation level is greater than the bond dissociation energy, the excited polymer dissociates into free radical fragments that can then further react to produce chain scission or polymer crosslinking. The energy associated with wavelengths of light commonly employed in lithography gradually increases as the wavelength is decreased, going from 115 kcal/mole to 147 kcal/mole to 182 kcal/mole at 248, 193, and 157 nm respectively. This level of energy can be compared with typical carbon-carbon bond dissociation energies of 90 to 120 kcal/mole implying that significant bond breaking photochemistry occurs.

The insertion of EUV, with a 13.4 nm wavelength, into the lithographic roadmap greatly increases the energy available for deposition into the resist polymer to 2133 kcal/mole. The higher energy associated with EUV coupled with the higher absorbance for most organic polymers at EUV should lead to increased excited state population and higher quantum yields of photoproducts. The pathway in which different polymers respond to this light energy, be it chain scission or crosslinking, will determine in large part the ability of resists designed at 193 or 248 nm to operate as EUV resists.

Advances in Resist Materials and Processing Technology XXVII, edited by Robert D. Allen, Mark H. Somervell,
Proc. of SPIE Vol. 7639, 76390A · © 2010 SPIE · CCC code: 0277-786X/10/$18 · doi: 10.1117/12.845997

Polymer absorbance of EUV radiation is also expected to produce low energy electrons that can interact with both polymer and PAG molecules. The nature of this phenomenon can be complex due to the variation in distribution of electron energies produced from EUV photon absorption and the different travel distances of the various energy electrons. In addition to direct EUV induced polymer photochemistry, there also exists the expectation of concurrent polymer main chain scission, side chain elimination, and crosslinking occurring from EUV-induced low energy electrons. The effect of the relatively large amounts of photo-induced polymer radicals on polymer photochemistry may lead to effective quantum yields far in excess of those reported for other optical lithographic wavelengths.

Polymers representative of those commonly employed in resists as well as some model polymers were selected for this study. Polymer photochemistry at EUV was catalogued as to the effect of absorbed 13.4 nm radiation on a polymer's propensity toward chain scission versus crosslinking. In selected cases, the chain scission and crosslinking quantum yields were also compared to those previously determined at 157, 193 and 248 nm. Quantum yields were determined by following the change in molecular weight, both number average (M_n) and weight average (M_w) molecular weight as a function of different absorbed doses, D, by a GPC (gel permeation chromatography) method. Solving Equations [1] and [2] simultaneously allows both Φ_s and Φ_x to be determined.

$$1 / M_{n,D} = 1 / M_{n,0} + [\Phi_s - \Phi_x] * D / NA \quad (1)$$

$$1 / M_{w,D} = 1 / M_{w,0} + [\Phi_s / 2 - 2\,\Phi_x] * D / NA \quad (2)$$

In the case where molecular weight decreases, it is important to determine if material outgassing is occurring and whether the outgassing occurs from small molecular weight fragments caused by chain scission or by side chain fragmentation. The nature of the material loss was determined for selected polymers where chain scission and material loss are significant. This knowledge can be used to design polymers that minimize undesired photochemical transformations and reduce material outgassing.

2. EXPERIMENTAL

The poly(hydroxystyrene-co-t-butylacrylate) polymers were obtained from DuPont Electronic Polymers[6] in molar ratios of 65:35 poly(hydroxystyrene-co-t-butylacrylate) (Poly-E3) and 50:50 poly(hydroxystyrene-co-t-butylacrylate) (Poly-E2). Poly(methyl methacrylate) (PMMA), poly(t-butylacrylate) (PTBA), and poly(hydroxystyrene)) (PHOST), were purchased from Aldrich Chemical.[6] Polymer solutions were prepared of 6% polymer in ethyl lactate for PHOST, Poly-E2 and PolyE3, in PGMEA for PMMA, and in toluene for PTBA.

All lithographic substrates were HMDS treated 100 mm silicon wafers except for samples employed for FTIR measurements which were 100 nm of evaporated aluminum on 100 mm silicon wafers. Polymer films were coated to 125 nm by spin casting followed by a post apply bake of 130°C for 60 s.

Samples were exposed to EUV radiation at Beamline 1 of the Synchrotron Ultraviolet Radiation Facility (SURF III) electron storage ring. The beamline is described fully in previous publications.[7,8] Briefly, radiation from SURF III is collected by a spherical Mo/Si multilayer mirror and focused to a sub-mm spot. Downstream from this, the expanding beam passes through a Zr filter that is captured in the gate of a gate valve. The filter serves three purposes: a spectral purity filter, eliminating DUV radiation that reflects from the mirror; a vacuum seal to prevent outgassing from the polymers from upstreaming and damaging critical components; and a beam-shaping aperture to ensure uniform exposure of the samples.

Preliminary exposures were made to determine the appropriate dose ranges prior to making full-wafer exposures. For these preliminary measurements, a circular free-standing filter is used, and a 3 mm aperture is placed 5 mm in front of the sample. The wafer is mounted 25 mm off-center and rotated to make multiple exposures on a single wafer. Full-wafer exposures are made using a mesh-backed triangular filter with the wafer continuously rotating. To maintain a reasonable throughput yet make the exposure as uniform as possible, a custom-designed mask is placed in front of the wafer. This makes the exposure uniform over the surface within 10% based on measurements made with an EUV-sensitive scintillator. To determine absolute incident intensity, the power was measured behind the 3 mm aperture with a calibrated photodiode. The uncertainty in the photodiode calibration is 1%. The uncertainty in the machining and measurement of the apertures is 5%, leading to a root-sum-square uncertainty in the exposure of 11%.

The rate of film thickness loss (FTL_{Dose}) was determined by determining the slope of a linear fit of the film thickness versus the exposure dose. The reported values are for an exposure dose of 100 mJ/cm^2. Film thickness

measurements were made at least 24 hours after exposure to ensure that all material outgassing was complete. Film solubility with exposure was performed by immersion in tetrahydrofuran (THF), an organic solvent, for 30 seconds.

The polymer quantum yield for both polymer chain scission and polymer crosslinking were determined from a slope of a least squares fit of inverse polymer molecular weight (both M_n and M_w) as a function of absorbed dose. The organic film of interest was spin cast to approximately 125 nm onto the silicon wafer followed by exposure of the entire wafer with EUV at the desired dose. Typically 9 wafers were exposed at different equally spaced doses ranging from 0 to 200 mJ/cm^2 for PMMA, 0 to 100 mJ/cm^2 for PHOST, 0 to 48 mJ/cm^2 for Poly-E2, and 0 to 32 mJ/cm^2 for PTBA and Poly-E3. After exposure the resist was stripped off the wafer in THF and the resulting solution concentrated to dryness. The dry film was resolubilized in 0.15 ml of THF and the molecular weight of the polymer was determined by gel permeation chromatography (GPC) relative to poly(methyl methacrylate) or polystyrene standards as appropriate. All molecular weights were determined in duplicate runs.

EUV absorbance was calculated from the Center for X-Ray Optics at Lawrence Berkeley National Laboratory web site by inputting the calculated polymer molecular formula and assuming a polymer density of 1.19 for the hydrocarbon polymers. EUV reflectance was assumed to be 0.1% for all samples based on previously published measurements of PMMA reflectivity.[9] Calculated values used for polymer absorbance (in base 10) are PHOST (1.78), Poly-E3 (1.88), Poly-E2 (1.92), PTBA (1.99), and PMMA (2.35).

Fourier transformed-infrared (FT-IR) measurements were made with a Bruker Equinox 55 FT-IR[6] employing an IRscope II in reflectance mode through a grazing angle objective. Polymer thickness was 125 nm on aluminum coated silicon wafers, spectral resolution was 4 cm^{-1} and typically 64 spectra were averaged from each exposure measurement. The Bruker Opus software which controlled the spectrometer data acquisition and IRscope II allowed one to measure a predetermined matrix of locations, which in our case corresponded to the location of the EUV exposure. The FT-IR reference signal was subtracted from the exposed area signal and integrated from 1710 cm^{-1} to 1750 cm^{-1}.

3. RESULTS AND DISCUSSIONS

Polymers representative of those commonly employed in 193 or 248 nm resists were selected for this study. General chemical structures of the polymers used are shown in Figure 1. Poly(hydroxystyrene) and poly(t-butyl methacrylate) were selected as a model polymers due to the use in many 248 nm based resists. Poly(methyl methacrylate) was selected as a model polymer for 193 nm resists. In addition to the above mentioned homopolymers, the quantum yields of several copolymers of hydroxystyrene and t-butyl acrylate were also determined.

The polymers selected for this study can undergo a number of potential photochemical transformations that lead to radical formation through either bond scission or hydrogen abstraction. Examples of these photochemical transformations are shown in Figure 2. Acrylate and methacrylate based polymers can undergo both Norrish Type 1 and Norrish Type 2 bond cleavage. A Norrish Type 1 cleavage occurs when the ester carbonyl is cleaved adjacent to the polymer main chain. This type of cleavage gives rise to an initial carbon radical on the polymer main chain which can then undergo further reactions that lead to polymer crosslinking. A Norrish Type 2 cleavage occurs when the polymer main chain cleaves leading to two new polymer chains of decreased molecular weight. Methacrylate polymers tend to favor Norrish Type 2 cleavages while acrylate polymers favor Norrish Type 1 cleavage. In addition, both polymer types are known to undergo ester elimination which may be followed by subsequent loss of carbon dioxide. Styrene based polymers normally undergo a bond scission reaction which leads again to an initial carbon radical on the polymer main chain which can then undergo further reactions that lead to polymer crosslinking.

The final photochemical reaction products will depend on the product of the reaction quantum yield and the amount of absorbed incident dose. The amount of polymer backbone chemistry can vary considerably between the three optical lithographic wavelengths, as both higher absorbance and increased quantum yield at lower wavelengths act in concert to yield an increased level of polymer backbone chemistry. At the EUV wavelength, the absorbance of all five of the model polymers are similar ranging from 1.78 to 2.35 μm^{-1} so that polymer absorbance will not be as significant of a driver of polymer photochemistry as it is at optical wavelengths. Instead at the EUV wavelength, the degree in which different polymers respond to this light energy and the pathway in which the photochemical reaction leads, be it chain scission or crosslinking, will determine the final photochemical reaction products. And it is these photochemical reaction products and their effect on resist properties such as deprotection kinetics and film dissolution that in large part determine the ability of polymers designed for 193 or 248 nm resists to be employed in EUV resists.

3.1 Polymer thickness change with EUV exposure

In order to determine the proper exposure dose range for determining the polymer quantum yield a set of preliminary experiments were performed in which a 125 nm thick polymer film was exposed to EUV at a series of doses up to 200 mJ/cm^2 and the film thickness remaining as a function of exposure dose was determined both after exposure and after immersion in THF. Figure 3 shows the resulting film thickness both after exposure and after exposure and THF development for poly(hydroxystyrene) and poly(methyl methacrylate). The poly(hydroxystyrene) shows virtually no film thickness loss up to 200 mJ/cm^2 while the poly(methyl methacrylate) exhibits about 9 nm of film loss with a 200 mJ/cm^2 exposure dose. The film loss of PMMA is consistent with some combination of radical induced ester elimination and Norrish Type 2 bond cleavage with the expectation that the less favored Norrish Type 1 bond cleavage will not predominate with methacrylate based esters.

Figure 3 also shows the retained polymer film thickness after THF development. The lack of retained film for PMMA with a 200 mJ/cm^2 exposure dose shows that no polymer crosslinking occurs up to this dose. This is contrasted with the results for PHOST where 40% of the film is retained at an exposure dose of 150 mJ/cm^2. The presence of any level of retained film strongly implies that crosslinking is occurring during exposure and that with exposure doses greater than 100 mJ/cm^2 the crosslinking is so great that the film is no longer soluble in THF. As THF is the solvent employed for GPC analysis, this limits the exposure dose that can be used on PHOST films exposed for GPC analysis to no greater than 100 mJ/cm^2.

A similar set of experiments was performed for the three other model polymers except that the exposure dose range was increased to a series of doses up to 330 mJ/cm^2 and the film thickness remaining as a function of exposure dose determined both after exposure and after immersion in THF. Figure 4 shows the resulting film thickness both after exposure and after exposure and THF development for poly(t-butyl acrylate) and two copolymers of t-butyl acrylate and hydroxystyrene in different monomer ratios, Poly-E2 and Poly-E3. All three polymers show film loss with exposure with the PTBA having the greater loss while the two copolymers have approximately equal film loss throughout the exposure range.

Figure 4 also shows the retained polymer film thickness after THF development. All three t-butyl acrylate containing polymers exhibit THF insolubility at much lower doses than the PHOST polymer. The PTBA and Poly-E3 are insoluble after only 44 mJ/cm^2 of EUV exposure while the Poly-E2 is insoluble after 66 mJ/cm^2 of EUV exposure. This limits the exposure dose range for all three polymers to values lower then the dose that first gives film insolubility. It is surprising that PTBA and the t-butyl acrylate containing copolymers become insoluble in THF at much lower doses than PHOST. This could be explained by two possible mechanisms. The t-butyl acrylate containing polymers can either have a very high quantum yield for crosslinking with EUV exposure or ester cleavage followed by carbonyl loss could be leading to a nonpolar polyethylene-like polymer that is not soluble in THF. The following section will investigate these possibilities.

3.2. Polymer quantum yield of chain scission and crosslinking with EUV exposure

The polymer quantum yield for chain scission and crosslinking were determined by coating 125 nm of the polymer film on a silicon wafer. The absorbances of the films at EUV, shown in Table 1, were such that the average optical density was about 0.25. This leads to a small nonuniformity in available dose as a function of depth into the polymer as the polymer at the silicon interface receives approximately three quarters of the dose as the polymer at the film surface. Although we calculate the total dose absorbed in the film, taking into account the change in absorbance as a function of film depth, the change in molecular weight determined by GPC is a change based on the average exposure dose. This will introduce some line broadening into the GPC molecular weight determination, but should not greatly affect the molecular weights determined.

A typical experiment to determine polymer quantum yield is shown in Figure 5 when the number average (M_n) and weight average (M_w) molecular weights of PMMA are plotted versus EUV exposure dose. All molecular weights were determined in duplicate runs. The PMMA M_n and M_w decrease rapidity with increasing dose, a result typical of that observed when chain scission is occurring. The molecular weight versus dose plot is then transformed to a plot of inverse molecular weight versus dose in photons per gram which is shown in Figure 6. The slope of the linear fit of inverse molecular weights, for both M_n and M_w, versus dose is determined and substituted into Equations 1 and 2 to determine the quantum yields of chain scission and crosslinking with EUV exposure. The quantum yields for chain scission and crosslinking for the five model polymers, including a duplicate determination of quantum yields for PHOST, are shown in Table 1.

Table 1. Summary of EUV absorbance, slope of inverse molecular weight versus dose, and quantum yields of polymers.

		Slope v. dose				
Polymer	**A (μm^{-1})**	**$1/M_n$**	**$1/M_w$**	**Φ_S**	**Φ_X**	**FTL_{100} ($nm/mJcm^{-2}$)**
PMMA	2.35	0.950	0.305	1.064	0.114	4.31
PHOST	1.78	-0.064	-0.136	0.005	0.072	0.22
PHOST	1.78	-0.139	-0.158	0.000	0.061	
Poly-E3	1.88	-0.148	-0.268	0.000	0.130	1.71
Poly-E2	1.92	-0.151	-0.214	0.000	0.092	2.62
PTBA	1.99	0.006	0.005	0.089	0.019	12.62

PMMA has an exceedingly high quantum yield of chain scission of 1.064 and a surprisingly high quantum yield of crosslinking of 0.114. A chain scission value approaching or greater than 1.0 often implies a radical chain mechanism to account for the high quantum yield value, although with the known propensity of EUV to generate secondary electrons in organic films, the possibility can not be ruled out that secondary electrons are responsible for the high quantum yield value for chain scission. The high value of crosslinking for PMMA is more difficult to explain in that methacrylate polymers are expected to undergo only chain scission and not undergo crosslinking. One can only speculate that the very energetic EUV photons are initiating sufficient bond breaking that some termination steps result in crosslinking events. It is noted that the combination of a very high level of chain scission coupled with the lower level of crosslinking for PMMA does not lead to a THF insoluble material but instead will give a lower molecular weight PMMA polymer that contains a high degree of branching.

PHOST has an expected moderately high value for the quantum yield of crosslinking with values of 0.072 and 0.061 determined in two separate experiments. PHOST is expected to crosslink and the results confirm that only crosslinking is occurring. PHOST is not expected to undergo chain scission and the two values for the quantum yield of chain scission at 0.005 and 0.000 are consistent with that expectation. Quantum yield values of less than 0.01 can be effectively considered zero so that both values determined for chain scission are consistent in showing that no chain scission of PHOST occurs under EUV exposure.

PTBA shows both a moderately high value of chain scission and also that crosslinking occurs with EUV exposure. This is surprising in that most acrylate based polymers undergo crosslinking and not chain scission. A possible explanation for this observation resides in the nature of GPC molecular weight determination. The GPC technique relies on the hydrodynamic volume of the polymer being related to the polymer molecular weight. This relationship holds true if the only photo-induced reactions are those that lead to molecular weight changes, but it breaks down if other photo-induced reactions occur that change the hydrodynamic volume of the polymer. If a sufficient amount of t-butyl ester elimination was occurring to change the hydrodynamic volume of the polymer, the GPC could erroneously measure a molecular weight decrease associated with chain scission and lead to incorrect determination of chain scission and crosslinking quantum yields. We believe that this is occurring and will present evidence for a large degree of ester elimination.

The Poly-E3 and Poly-E2 behave similarly in that both exhibit relatively high quantum yield values for crosslinking and show no chain scission. Past work has shown that the presence of aromatic groups in the polymer will inhibit chain scission[3,4] and this effect is also seen with EUV exposure. The value for quantum yield for crosslinking between PHOST, PTBA, and the two copolymers shows no trend as to the relative amount of either hydroxystyrene or t-butyl acrylate in the polymer.

An indication that significant ester cleavage is occurring can be seen in Table 1 where the film thickness loss at 100 mJ/cm^2 (FTL_{100}) is calculated for all five polymers. The film thickness loss is likely predominately caused by ester cleavage either at the ether linkage or by complete decarboxylation of the ester and should be a good indicator of the degree of ester cleavage. The PHOST has the lowest FTL_{100} of 0.22 while PMMA, which is known to decarboxylate, has a relatively high FTL_{100} value of 4.31. The PBTA has the highest value at 12.62 showing significant film loss and

expected ester decarboxylation. Interestingly, the two copolymers show FTL_{100} values intermediate of those of the homopolymers although much suppressed compared to what would be predicted simply by the relative amount of t-butyl acrylate in the copolymer although the copolymer having the higher level of aromatic content gives the lower amount of film loss.

3.3 Polymer photochemistry monitored by FTIR

In order to further elucidate the degree of polymer decarboxylation with EUV exposure, the carbonyl absorbance of ester based polymers was determined by FTIR as a function of EUV exposure dose by integrating the FTIR spectra from 1710 cm^{-1} to 1750 cm^{-1}. The highest level of exposure dose employed, either 200 mJ/cm^2 for PMMA or 330 mJ/cm^2 for the acrylate containing polymers, did not give full removal of the carbonyl absorbance. This did not allow the determination of a baseline integration value for the 1710 cm^{-1} to 1750 cm^{-1} region with complete removal of carbonyl and as such the normalized amount of carbonyl present could not be determined, so only the relative integrated values of carbonyl absorbance are reported.

Figure 7 shows the FTIR spectra of PMMA with different levels of EUV exposure (the different spectra are offset for clarity). The FTIR absorbance peak of most interest occurs between 1710 cm^{-1} to 1750 cm^{-1} and is associated with the carbonyl absorbance of the methyl ester. It can be seen that the peak height decreases with increasing EUV dose although even at the highest EUV dose investigated a strong carbonyl peak is still present. Although peak height is an indicator of concentration, the preferred measure of concentration from FTIR is peak area integration and Figure 8 shows the integrated area absorbance from 1710 cm^{-1} to 1750 cm^{-1} as a function of exposure dose.

The value of the integrated absorbance decreases with increasing exposure dose for PMMA indicating that ester decarboxylation is occurring as a function of exposure dose although as stated earlier the actual amount of ester decarboxylation can not be determined since a baseline absorbance value for complete ester removal was not determined. A second observation is that the level of decarboxylation appears to occur in two distinct regions. A linear fit of integrated absorbance to exposure dose does not fully describe the change in integrated absorbance. Instead the decarboxylation appears to have two distinct regions depending on the exposure dose. At exposure values from 0 to 20 mJ/cm^2, a relatively steep slope is observed which decreases at exposure doses greater than 20 mJ/cm^2. This could imply that two decarboxylation mechanisms are occurring under EUV radiation.

Figure 9 shows the 1710 cm^{-1} to 1750 cm^{-1} region integrated absorbance for the three acrylate containing polymers with EUV exposure. Again, the level of decarboxylation appears to occur in two distinct regions, with a higher slope region occurring between 0 to 50 mJ/cm^2 and a low slope region occurring after 50 mJ/cm^2. It is clear from the results shown in Figures 8 and 9 that significant decarboxylation occurs in the methacrylate and acrylate polymers at relatively low EUV doses and that this decarboxylation will fundamentally change the nature of the polymer and its associated dissolution characteristics.

The decarboxylation can also affect the molecular weight determinations performed by GPC in that the GPC technique relies on the hydrodynamic volume of the polymer being related to the polymer molecular weight. The t-butyl ester elimination that occurs can change the hydrodynamic volume of the polymer leading to an erroneously measured molecular weight decrease and resulting in higher levels of measured chain scission than actually occur.

3.4 Comparison of polymer photochemistry at different wavelengths

The quantum yields and film thickness loss of the model polymers can be compared to values previously determined at more traditional optical wavelengths of 157, 193, and 248 nm. Table 2 summarizes the quantum yields of scission and crosslinking from previously published work along with the values reported herein.[4,5] It can be seen that PMMA does have a propensity to undergo crosslinking at EUV although not at other wavelengths and that the level of chain scission is greatly increased relative to the optical wavelengths. PHOST undergoes only crosslinking at EUV but again at rate far greater then seen at optical wavelengths. The three acrylate containing polymers generally behave similarly at EUV and optical wavelengths although again the EUV quantum yields are often an order of magnitude or more greater than at optical wavelengths. Thus EUV radiation not only greatly increases the magnitude of the polymers propensity toward chain scission or crosslinking, but unlike optical wavelengths, it also shows crosslinking with non-aromatic homopolymers.

Table 2. Summary of quantum yield of chain scission and crosslinking at different lithographic wavelengths.

	13.4 nm		157 nm		193 nm		248 nm	
Polymer	Φ_S	Φ_X	Φ_S	Φ_X	Φ_S	Φ_X	Φ_S	Φ_X
PMMA	1.064	0.114	0.019	0.000	0.014	0.000	0.032	0.000
PHOST	0.005	0.072	0.000	0.012			0.000	0.006
PHOST	0.000	0.061	0.000	0.012			0.000	0.006
Poly-E3	0.000	0.130	0.000	0.009			0.000	0.001
Poly-E2	0.000	0.092	0.000	0.006				
PTBS	0.089	0.019	0.005	0.000	0.003	0.000	0.003	0.000

Figure 10 shows the normalized film thickness loss of PMMA exposure with different wavelengths plotted against the number of absorbed photons instead of the traditional method of plotting versus energy dose. This method is preferred when comparing wavelengths of such differing photon energies and film absorbencies in that it only addresses the number of photons that actually are absorbed in the polymer film. Figure 10 clearly shows that the three optical wavelengths have similar slopes indicating that the film loss generally follows the degree of absorbed photon. This is not surprising given the similar energies of the photons ranging from 115 to 182 kcal/mole. What is surprising is that the much more energetic EUV photon, 2133 kcal/mole, gives a much shallower slope showing that many times more absorbed photons are required to give film loss presumably via ester elimination and decarboxylation.

Figures 11 and 12 show similar trends in that the slopes of the three optical wavelengths are much steeper than that of the EUV slope when tracking normalized film loss versus absorbed photons for the acrylate containing polymers. Again many times more photons are required with EUV to give film loss than with optical wavelengths. It could be argued that EUV with its ability to generate secondary electrons would be expected to give a greater amount of film loss per absorbed photon due to any additional film loss resulting from secondary electrons, but this is clearly not the case that is observed.

Instead one can speculate that at optical wavelengths where the photon absorption occurs primarily in functional groups, such as the ester carbonyl, the energy is deposited directly in the functional group that will undergo the photochemical transformation. This could lead to a higher ester elimination reaction, possibly at the expense of chain scission or crosslinking. EUV absorbance can be considered atomic absorbance and will be distributed throughout the atoms of the polymer and not localized on the functional groups. This could account for the lower film loss at EUV and also the significantly higher quantum yields due to energy deposition directly onto the main polymer chain although secondary electrons could also assist in increasing both chain scission and croslinking quantum yields.

4. CONCLUSIONS

We have extended our technique for determining quantum yields of chain scission and crosslinking of polymer films coated on silicon wafers to EUV wavelengths. Model polymers selected to represent those commonly employed in 193 nm resists, PMMA, or 248-nm resists, PHOST and TBA, were selected for this study as were two copolymers of hydroxystyrene and t-butyl acrylate. It was shown that, except for PHOST, significant film loss occurs with exposure doses between 20 and 50 mJ/cm^2 and that the film loss is primarily the result of ester elimination and subsequent decarboxylation. It was also shown that less film loss occurs with EUV than with optical wavelengths per absorbed photon. It was speculated that the reason for this is that the atomic absorbance of EUV was less likely to deposit energy into the carbonyl group than the functional group absorbance of the optical wavelengths.

The quantum yield of chain scission and crosslinking were considerably higher with EUV versus optical wavelengths. In addition some polymers exhibited photochemistry not observed at optical wavelengths. PMMA and PTBA both showed crosslinking at EUV that was not seen at the optical wavelengths. Finally, the polymer photochemistry differences at EUV must be considered when designing resists for EUV based on polymers originally designed for optical wavelengths. The unexpected high level of crosslinking seen with PMMA at EUV could portend even higher levels of crosslinking with the common methacrylate based polymers employed in 193 nm resists. Equally disturbing is the high level of the decarboxylation reaction that occurs at EUV, which will fundamentally change the

nature of the polymer and its associated dissolution characteristics. Thus EUV initiated polymer photochemistry much be considered in EUV resist design.

5. ACKNOWLEDGEMENT

The Lincoln Laboratory portion of this work was sponsored by a Cooperative Research and Development Agreement between Lincoln Laboratory and Intel Corporation. The NIST portion of this work was supported in part by Intel. Opinions, interpretations, conclusions, and recommendations are those of the authors and are not necessarily endorsed by the United States Government.

We would like to acknowledge Todd Younkin of Intel for technical discussions and insights. We would also like to thank Michael Sheehan and Matt Romberger of DuPont Electronic Polymers for providing the polymers used in this study.

6. REFERENCES

[1] Roberts, J., Bacuita, T., Bristol, R., L., Cao, H., Chandhok, M., Lee, S., H., Leeson, M., Liang, T., Panning, E., Rice, B., J., Shah, U., Shell, M., Yueh, W. and Zhang, G., "Exposing extreme ultraviolet lithography at Intel," *Microelectronic Engineering* **83**, 672 (2006).

[2] Putna, E., S., Younkin, T., R., Chandhok, M. and Frasure, K., "EUV Lithography for 30nm Half Pitch and Beyond: Exploring Resolution, Sensitivity and LWR Tradeoffs," *Proc. SPIE* **7273**, 72731L (2009).

[3] Fedynyshyn, T., H., Goodman,R., B. and Roberts, J.,"Polymer Matrix Effects on Acid Generation," *Proc. SPIE* **6923**, 692319, (2008).

[4] Fedynyshyn, T., H., Kunz, R., R., Sinta, R., F., Goodman, R., B. and Doran, S., P., "Polymer Photochemistry at Three Advanced Optical Wavelengths", Forefront of Lithographic Materials Research: Proc. of International Conference on Photopolymers **12**, 3 (2000).

[5] Fedynyshyn, T., H., Kunz, R., R., Sinta, R., F., Goodman, R., B. and Doran, S., P., "Polymer photochemistry at advanced optical wavelengths," *J. Vac. Sci. Technol. B* **18**, 3332 (2000).

[6] "Product names or brands are mentioned only for experimental completeness. This does not constitute endorsement by NIST or the Federal Government."

[7] Tarrio, C. and Grantham, S., "A synchrotron beamline for extreme-ultraviolet multilayer mirror endurance testing," *Rev. Sci. Instrum*. **76**, 056101 (2005)

[8] Tarrio, C., "Method for the characterization of extreme-ultraviolet photoresist outgassing," *J. Res. NIST* **114**, 179 (2009).

[9] Irie, S., Endo, M., Sasago, M., Kandaka, N., Kondo, H. and Murakami, K., "Measurement of resist transmittance at extreme ultraviolet wavelength using the extreme ultraviolet reflectometer," *Jpn. J. Appl. Phys.* **41,** 4027 (2002).

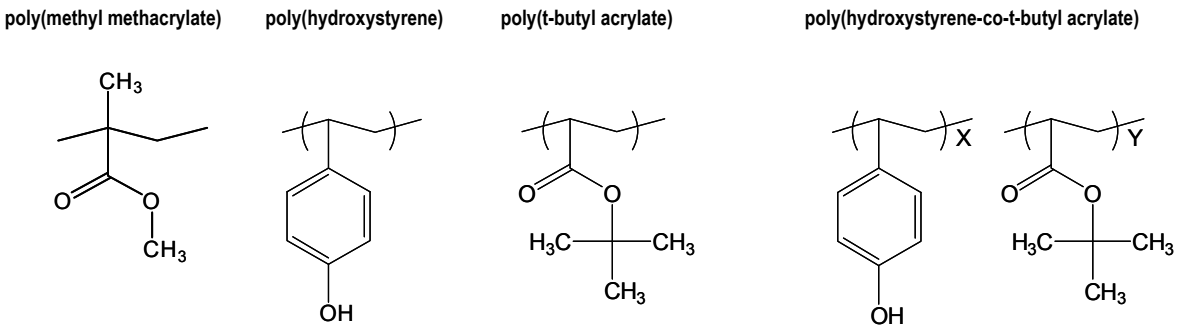

Figure 1. Chemical structures of homopolymers and copolymers.

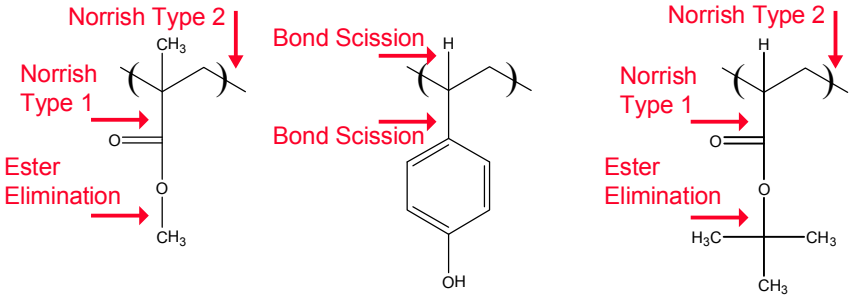

Figure 2. Photochemical bond cleavages that can occur with polymethyl methacrylate, polyhydroxystyrene and poly-t-butyl acrylate.

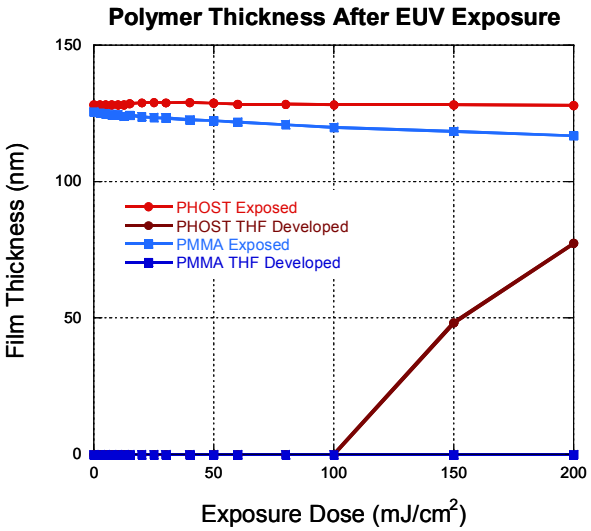

Figure 3. Film thickness loss with EUV exposure before and after THF development for poly(methyl methacrylate) and poly(hydroxystyrene)

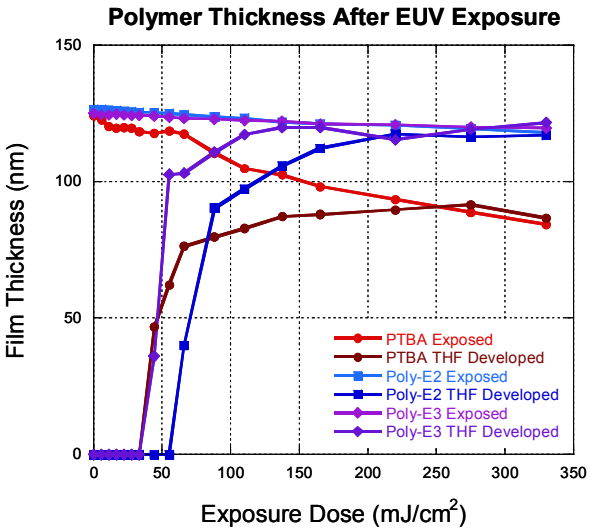

Figure 4. Film thickness loss with EUV exposure before and after THF development for poly(t-butyl acrylate) and two ESCAP copolymers.

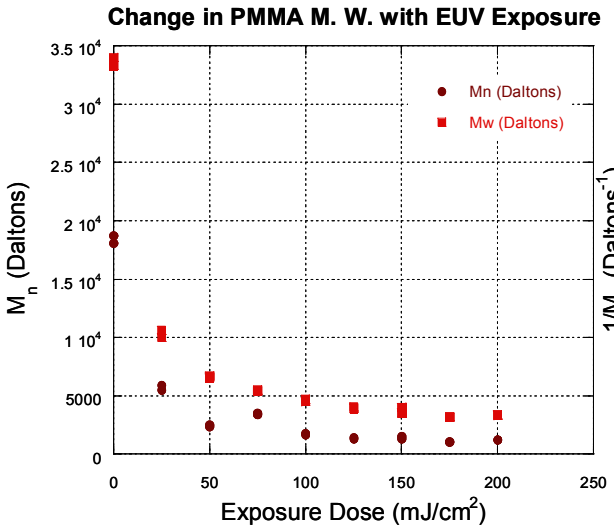

Figure 5. Change in molecular weight of poly(methyl methacrylate) as a function of EUV exposure dose.

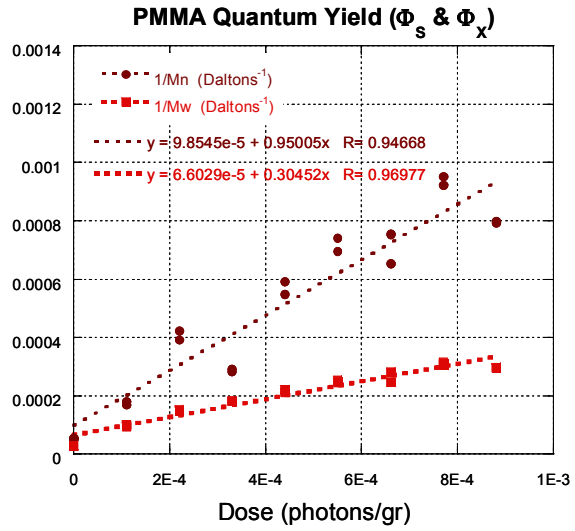

Figure 6. Determination of quantum yield of chain scission and crosslinking for poly(methyl methacrylate) with EUV exposure.

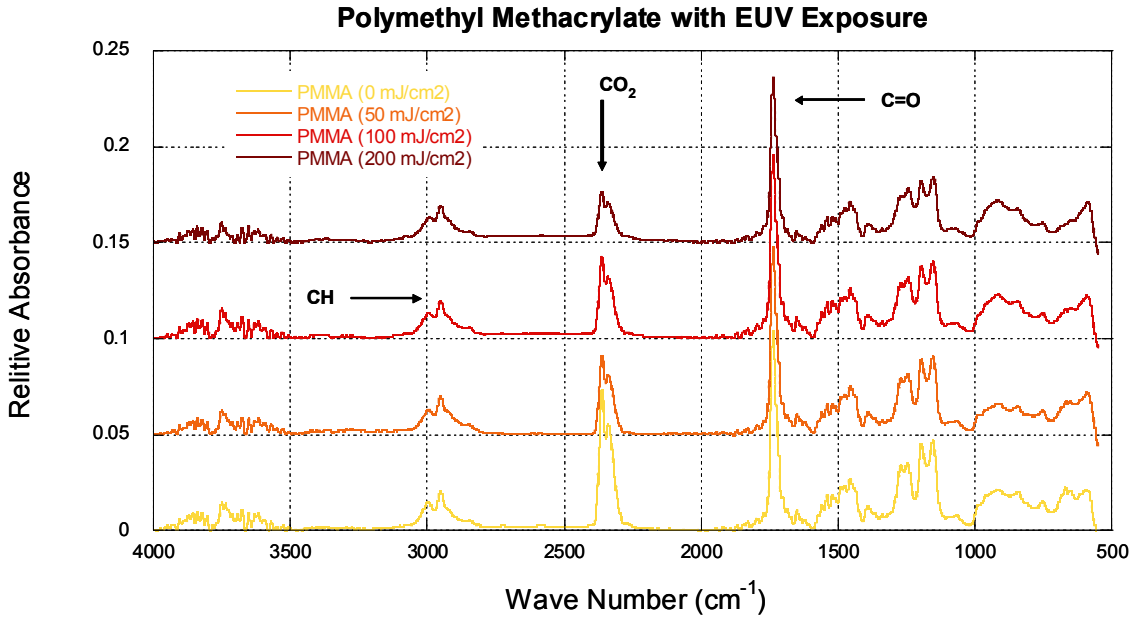

Figure 7. FTIR spectra of poly(methyl methacrylate) at different EUV doses showing a decrees of the carbonyl peak height with increasing dose.

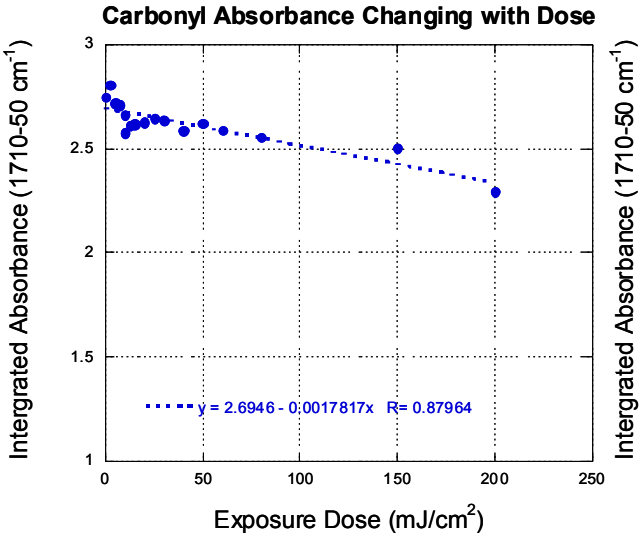

Figure 8. Integrated absorbance of the carbonyl peak of poly(methyl methacrylate) with EUV exposure dose and linear fit of absorbance v. dose.

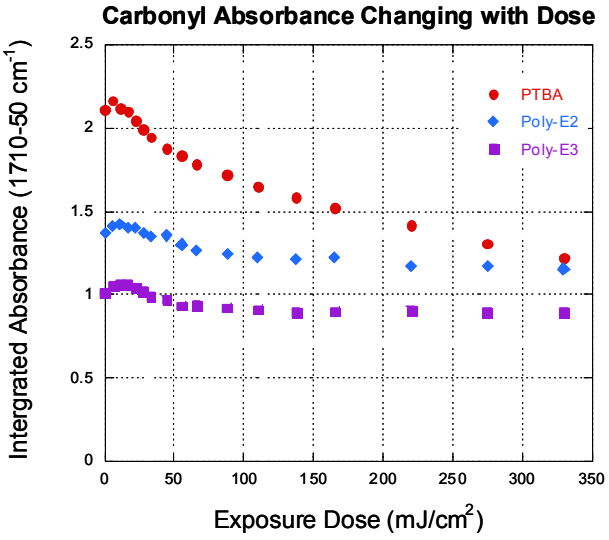

Figure 9. Integrated absorbance of the carbonyl peak of poly(t-butyl acrylate) and two ESCAP copolymers with EUV exposure dose.

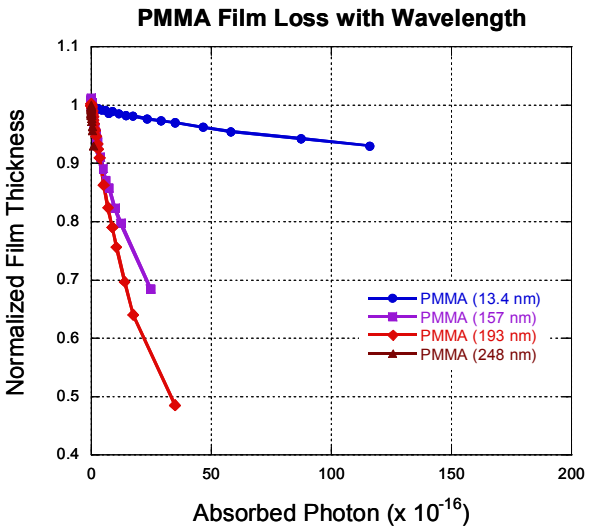

Figure 10. Normalized film loss with absorbed photon for poly(methyl methacrylate) with different lithographic exposure wavelengths.

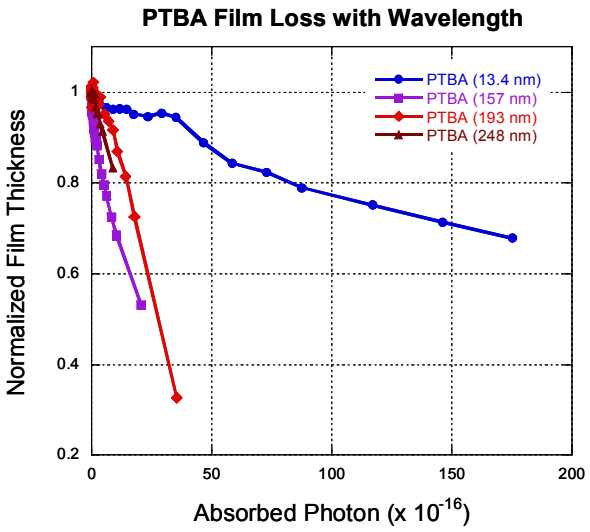

Figure 11. Normalized film loss with absorbed photon for poly(t-butyl acrylate) with different lithographic exposure wavelengths.

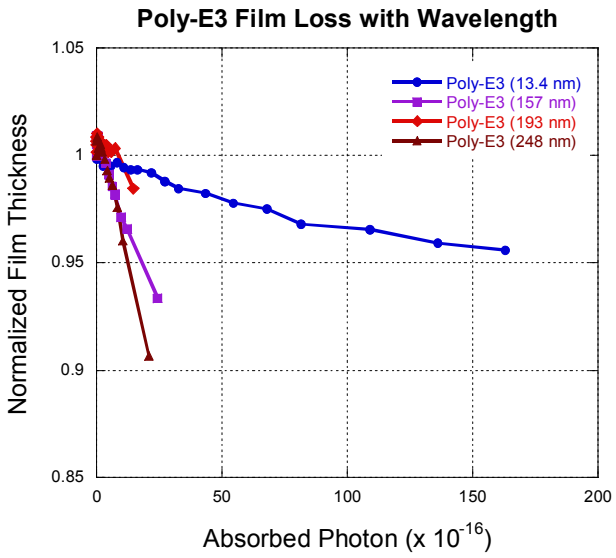

Figure 12. Normalized film loss with absorbed photon for Poly-E3 with different lithographic exposure wavelengths.